Continued increase of CFC-113a (CCl₃CF₃) mixing ratios in the global atmosphere: emissions, occurrence and potential sources

Karina E. Adcock[1], Claire E. Reeves[1], Lauren J. Gooch[1], Emma C. Leedham Elvidge[1],

Matthew J. Ashfold[2], Carl A. M. Brenninkmeijer[3], Charles Chou[4], Paul J. Fraser[5],

Ray L. Langenfelds[5], Norfazrin Mohd Hanif[1], Simon O'Doherty[6], David E. Oram[1,7],

Chang-Feng Ou-Yang[8], Siew Moi Phang[9], Azizan Abu Samah[9], Thomas Röckmann[10],

William T. Sturges[1], and Johannes C. Laube[1]

[1]Centre for Ocean and Atmospheric Sciences, School of Environmental Sciences, University of East Anglia, Norwich, NR4 7TJ, UK
[2]School of Environmental and Geographical Sciences, University of Nottingham Malaysia Campus, 43500 Semenyih, Malaysia
[3]Air Chemistry Division, Max Planck Institute for Chemistry, Mainz, Germany
[4]Research Center for Environmental Changes, Academia Sinica, Taipei 11529, Taiwan
[5]Commonwealth Scientific and Industrial Research Organisation, Oceans and Atmosphere, Climate Science Centre, Aspendale, Australia
[6]Department of Chemistry, University of Bristol, Bristol, UK
[7]National Centre for Atmospheric Science, School of Environmental Sciences, University of East Anglia, Norwich, NR4 7TJ, UK
[8]Department of Atmospheric Sciences, National Central University, Taipei, Taiwan
[9]Institute of Ocean and Earth Sciences, University of Malaya, Kuala Lumpur, Malaysia
[10]Institute for Marine and Atmospheric Research Utrecht, Utrecht University, Utrecht, the Netherlands

Correspondence to: Karina Adcock (Karina.Adcock@uea.ac.uk)

Abstract

Atmospheric measurements of the ozone depleting substance CFC-113a (CCl₃CF₃) are reported from ground-based stations in Australia, Taiwan, Malaysia and the United Kingdom, and aircraft-based measurements in the upper troposphere and stratosphere. Building on previous work we find that, since the gas first appeared in the atmosphere in the 1960s, global CFC-113a mixing ratios have been increasing monotonically to the present day. Mixing ratios of CFC-113a have increased by 40 % (percent) from 0.50 to 0.70 ppt (parts per trillion) in the Southern Hemisphere between the end of the previously published record in December 2012 and February 2017. We derive updated global emissions of 1.7 Gg yr⁻¹ (1.3-2.4 Gg yr⁻¹) on average between 2012 and 2016 using a two-dimensional model. We compare the long-term trends and emissions of CFC-113a to those of its structural isomer, CFC-113 (CClF₂CCl₂F), which still has much higher mixing ratios than CFC-113a, despite its mixing ratios and emissions decreasing since the 1990s. The continued presence of Northern Hemispheric emissions of CFC-113a is confirmed by our measurements of a persistent interhemispheric gradient in its mixing ratios, with higher mixing ratios in the Northern Hemisphere. The sources of CFC-113a are still unclear, but we present evidence that indicates large emissions in East Asia, most likely due to its use as a chemical involved in the production of hydrofluorocarbons. Our aircraft data confirm the interhemispheric gradient as well as showing mixing ratios consistent with ground-based observations and the relatively long atmospheric lifetime of CFC-113a. CFC-113a is the only known CFC for which abundances are still substantially increasing in the atmosphere.

1. Introduction

The ozone layer in the stratosphere blocks harmful ultraviolet radiation from reaching the Earth's surface and therefore protects human health and the environment. Chlorofluorocarbons (CFCs) are industrially produced chemicals that were commonly used as refrigerants, aerosol propellants, solvents and foam blowing agents. These compounds act as catalysts in the destruction of ozone and they have, in combination with other chlorine and bromine containing gases, led to the formation of the ozone hole (Farman et al., 1985; Molina and Rowland, 1974). The discovery of this phenomenon motivated the `Montreal Protocol on Substances that Deplete the Ozone Layer', an international agreement to phase out the use of CFCs and other ozone depleting substances (ODSs) (UNEP, 2016a). It came into force in 1989 and, other than for a few critical use exceptions, there has been a global ban on CFC production since 2010 (UNEP, 2016a). Due to this, mixing ratios of most CFCs are now decreasing in the atmosphere and the ozone hole shows signs of recovery (Pawson et al., 2014; Solomon et al., 2016). Continued reductions in CFC mixing ratios are needed to allow the ozone layer to recover to pre-1970 levels.

Recently, mixing ratios of CFC-113a (CCl_3CF_3), the structural isomer of the well-known ozone-depleting substance CFC-113 ($CF_2ClCFCl_2$), were found to still be increasing in the atmosphere up until 2012 (Laube et al., 2014). The previously published evidence for increasing mixing ratios of CFC-113a comes from air samples collected at Cape Grim, Tasmania (41° S) and firn air data collected in Greenland (77° N) in 2008 (NEEM project) (Buizert et al., 2012; Laube et al., 2014). The firn air depth profile data, when combined with inverse modelling, provide smoothed time series of compound mixing ratios going back up to a century (Buizert et al., 2012; Laube et al., 2012). CFC-113a became detectable in the atmosphere in the 1960s (Laube et al., 2014). Cape Grim is a clean-air measurement site located in Tasmania, Australia, with air sampling/analysis activities since 1976 and the CFC-113a record derived from the Cape Grim Air Archive (1978 onwards) shows mixing ratios increasing over time with a sharp acceleration starting around 2010 (Laube et al., 2014). Global annual emissions of CFC-113a were estimated using a two-dimensional atmospheric chemistry-transport model, showing increases since the 1960s and more than doubling between 2010 and 2012, reaching 2.0 Gg yr^{-1} in 2012 (Laube et al., 2014). In addition, measurements of aircraft samples from the IAGOS-CARIBIC project identified an interhemispheric gradient with mixing ratios increasing from the Southern Hemisphere to the Northern Hemisphere; and the atmospheric lifetime of CFC-113a was estimated at 51 years from stratospheric research aircraft flights in late 2009 and early 2010 (Laube et al., 2014).

The origin of the emissions that cause this increase in CFC-113a mixing ratios is yet undetermined. Some evidence of a potential connection with hydrofluorocarbon (HFC) production has been found (Laube et al., 2014) and here we use additional data to investigate this possibility further. Laube et al. (2014) reported data until 2012. This paper uses data that have become available since 2012 to provide an update on its global trend and emissions and to assess these in terms of our understanding of the sources of this gas and its potential impact on ozone.

2. Methods

2.1 Analytical technique

Air samples from all the campaigns discussed in this study were collected in electropolished and/or silco-treated stainless steel gas cylinders, except for the CARIBIC project, for which samples were collected using a glass-bottle based sampler (Brenninkmeijer et al., 2007). After collection, the samples were transported to the University of East Anglia (UEA) to be analysed on a high-sensitivity gas chromatograph coupled to a Waters AutoSpec magnetic sector mass spectrometer (GC-MS). The trace gases were cryogenically extracted and pre-concentrated. A full description of this system can be found in Laube et al. (2010). Analysis was partly carried out using a GS GasPro column (length ~50 m, ID 0.32 mm) and partly with a KCl-passivated Al-PLOT column (length: 50 m, ID 0.32 mm, (Laube et al., 2016). The latter analysis has been slightly modified by the addition of an Ascarite filter to remove carbon dioxide. Several tests and comparisons ensured that no significant differences in CFC-113 and CFC-113a mixing ratios were obtained regardless of the column or filter used. The calibration scale used for CFC-113a is the UEA calibration scale and for CFC-113 is the NOAA 2002 calibration scale. The dry air mole fraction (mixing ratio) is measured and the units, parts per trillion (ppt) are used in this study as an equivalent to picomole per mole. The measurement uncertainties represent the one sigma standard deviation and are derived as the square root of the sum of the squared uncertainties from sample repeats and repeated measurements of an air standard on the same day.

2.2 Sampling

The following new data are presented in this study (see also Figure 1 and Table 1):

1. Laube et al. (2014) reported CFC-113a measurements from Cape Grim, Tasmania from 1978 to 2012. This paper reports four more years of CFC-113a measurements from Cape Grim, up to February 2017. The CFC-113 mixing ratios, 1978-2017, from the UEA Air Archive, NOAA flask data, and AGAGE in situ data are also included to compare the two isomers. The Cape Grim air samples were collected under background conditions with winds from the south-west, marine sector, so that sampled air masses were not influenced by nearby terrestrial sources and are representative of the large-scale Southern Hemisphere atmosphere. Details of the sampling procedure have been reported in previous publications (e.g. Fraser et al., 1999; Laube et al., 2013).

2. Tacolneston tower is a measurement site in Norfolk (Ganesan et al., 2015), and is part of the UK Tall Tower Network. Air samples were collected on a near-biweekly basis between July 2015 and March 2017 using an inlet at 185 m.

3. Ground-based samples were collected from Bachok Marine Research Station on the northeast coast of Peninsular Malaysia in January and February 2014.

4. During the StratoClim campaign (http://www.stratoclim.org/), air samples were collected during two flights by the Geophysica high altitude research aircraft, as described in Kaiser et al. (2006), in the upper troposphere and stratosphere (10-20 km) over the Mediterranean on 01/09/2016 and 06/09/2016.

5. Air samples were collected at regular intervals at altitudes of 10-12km during long distance flights on a commercial Lufthansa aircraft from 2009 to 2016 (Brenninkmeijer et al., 2007) on four flights between Frankfurt, Germany and Bangkok, Thailand; five flights between Frankfurt, Germany and Cape Town, South Africa; and one flight between Frankfurt, Germany and Johannesburg, South Africa; including the four flights referred to in Laube et al. (2014) (CARIBIC project, www.caribic-atmospheric.com).

6. Four ground-based air sampling campaigns took place in Taiwan from 2013 to 2016. Between 19 and 33 air samples were collected in March and April each year. In 2013 and 2015 samples were collected from a site on the southern coast of Taiwan (Hengchun) and in 2014 and 2016 samples were collected from a site on the northern coast of Taiwan (Cape Fuguei). See also Vollmer et al. (2015), Laube et al. (2016) and Oram et al. (2017). The median mixing ratios are used for the measurements made at the Taiwan sites to decrease the influence of the large spikes in CFC-113a mixing ratios that occurred during these campaigns (Section 3.2.1). All other averages are calculated using the mean.

2.3 Emission modelling

A two-dimensional atmospheric chemistry-transport model was used to estimate the top-down global annual emissions of CFC-113a and CFC-113. This model was previously used to estimate the global annual emissions of CFC-113a (Laube et al., 2014). In this study, the CFC-113a emission estimates are updated using an additional four years of Cape Grim measurements and CFC-113 emissions are estimated using CFC-113 mixing ratios at Cape Grim for 1978-2017 from the UEA Air Archive and compared with bottom-up emissions estimates from the Alternative Fluorocarbons Environmental Acceptability Study (AFEAS, https://agage.mit.edu/data/afeas-data). For further details see the supplementary material.

A latitudinal distribution of emissions, with 95 % of emissions originating in the Northern Hemisphere, was assumed for both compounds. As Cape Grim is an isolated Southern Hemispheric site the emission distribution within the Northern Hemisphere has almost no effect on the modelled mixing ratios in the latitudinal band Cape Grim is located in. The emissions distribution used for CFC-113 was assumed to be constant for the whole of the model run. This distribution has been used in previous studies for similar compounds (McCulloch et al., 1994; Reeves et al., 2005; Laube et al., 2014, 2016) and has been shown to reproduce the reported mixing ratios of CFC-11 and CFC-12 at Cape Grim to within 5 % uncertainty (Reeves et al., 2005). We decided to select an emission distribution for CFC-113a based on how well the modelled mixing ratios in the latitude band 48.6-56.4° N agreed with the observations at Tacolneston. Tacolneston can be considered to be representative of Northern Hemisphere background mixing ratios of CFC-113a as there are no large spikes in mixing ratios (Figure 2). The emission distribution used in the CFC-113a model is the same as CFC-113 for the first 60 years (1934-1993) and then

gradually shifts over the next 10 years from more northerly latitudes (36-57° N) to more southerly latitudes (19-36° N). It then remains at more southerly latitudes until the end of the run in 2017. This distribution shift is based on the assumption that CFC-113a emissions are predominantly from Europe and North America at the beginning of the model run and then shift to be coming predominantly from East Asia towards the end of the model run. The latter is consistent with our measurements from Taiwan (Section 3.2.1) and previous work has found that emissions of ozone depleting substances shifted from more northerly Northern Hemisphere latitudes to more southerly Northern Hemisphere latitudes (Reeves et al., 2005; Montzka et al., 2009). This is likely due to developing countries, which are mostly located further south, having more time to phase out the use of many ODSs than developed countries (Newland et al., 2013; CTOC, 2014; Fang et al., 2016). With this emissions distribution, the modelled CFC-113a mixing ratios at Tacolneston matched closely to the observations (Figure 2). It should be noted that while there is evidence that supports the emission distribution used here, there might be alternative distributions that result in equally good fits to the trends, particularly in the earlier part of the record.

2.4 Dispersion modelling

The UK Met Office's Numerical Atmospheric Modelling Environment (NAME, Jones et al. 2007), a Lagrangian particle dispersion model, was used to produce footprints of where the air sampled during the Taiwan and Malaysia campaigns (Table 1) had previously been close to the Earth's surface. The model setup related to samples collected in Taiwan in 2016 was slightly different to the setup for simulations in 2013-2015; hereafter those differences are noted in parentheses, though they have no practical implications for our findings. The footprints were calculated over 12 days by releasing batches of 60,000 (30,000 in 2016) inert backward trajectories over a 3 hour period encompassing each sample. Over the course of the 12 day travel time the location of all trajectories within the lowest 100m of the model atmosphere was recorded every 15 minutes on a grid with a resolution of 0.5625° longitude and 0.375° latitude (0.25° by 0.25° in 2016). The trajectories were calculated using three-dimensional meteorological fields produced by the UK Met Office's Numerical Weather Prediction tool, the Unified Model (UM). These fields have a horizontal grid resolution of 0.35° longitude by 0.23° latitude for the 2013 and 2014 simulations, and 0.23° longitude by 0.16° latitude for the 2015 and 2016 simulations. In all cases the meteorological fields have 59 vertical levels below ~30km.

3. Results

3.1 Long-term atmospheric trends and estimated global annual emissions of CFC-113a and CFC-113

CFC-113a atmospheric mixing ratios at Cape Grim were previously found to be increasing from 1978-2012 (Laube et al., 2014, Figure 3). Since 2012, CFC-113a mixing ratios at Cape Grim have continued to increase from 0.50 ppt in December 2012 to 0.70 ppt in February 2017 (Figure 3). Overall CFC-113a mixing ratios increased gradually until about 2010 followed by a more rapid increase. Between 1978 and 2009 CFC-113a mixing ratios increased on average by 0.012 ppt yr^{-1}; then between 2009 and 2017 they increased by about 0.037 ppt yr^{-1} i.e. more than three times the increase from the previous period.

Although measurements were made for a shorter time at Tacolneston (20 months), this site also shows an increase in CFC-113a mixing ratios of 0.03 ppt yr^{-1} over the period July 2015 to March 2017 (Figure 2). Furthermore, the median mixing ratios of CFC-113a in Taiwan increased on average by 0.06 ppt yr^{-1} from 2013 to 2016. During the CARIBIC flights the mean mixing ratios of CFC-113a increased on average, by 0.04 ppt yr^{-1} between 2009 and 2016. Overall, there is a consistent picture of a continued global increase in background mixing ratios of CFC-113a. It has been increasing since the 1960s (Laube et al., 2014) and continued to increase until early 2017; therefore there must be ongoing emissions of CFC-113a into the atmosphere. The modelled global annual CFC-113a emissions increased steadily at an average rate of 0.02 Gg yr^{-1} yr^{-1} until 2010 and then there was a sharp increase in the average growth rate to 0.52 Gg yr^{-1} yr^{-1} from 2010 to 2012 (Figure 3). We find that between 2012 and 2016, modelled emissions were on average 1.7 Gg yr^{-1} (1.3-2.4 Gg yr^{-1}). The best model fit suggests some minor and statistically non-significant variability between 1.6 and 1.9 Gg yr^{-1}.

It is instructive to look at CFC-113 to learn more about CFC-113a. The atmospheric trends and estimated emissions of CFC-113 at Cape Grim (Figure 4) are very different from those of CFC-113a. Mixing ratios of both

190 compounds increased at the beginning of the record, but then the CFC-113 mixing ratios stabilised in the early 1990s and then started to decrease (Figure 4), consistent with previous observations (Montzka et al., 1999; Rigby et al., 2013; Carpenter and Reimann, 2014). This trend is similar to those of many other CFCs in the atmosphere (for example CFC-11 and CFC-12, Rigby et al., 2013), but in contrast to the increasing mixing ratios of CFC-113a. Note that CFC-113 mixing ratios are still much higher than those of CFC-113a even at the end of our current record in early 2017. CFC-113 is the third most abundant CFC in the atmosphere (Carpenter and Reimann, 2014) and mixing ratios of CFC-113a are only about 1 % of CFC-113 mixing ratios in 2017. CFC-113 mixing ratios at

195 Cape Grim measured by NOAA (https://www.esrl.noaa.gov/gmd/dv/ftpdata.html) and AGAGE (http://agage.eas.gatech.edu/data_archive/agage/) are also included in Fig. 4. There is a small offset of 2 % between the NOAA data and the current UEA Cape Grim dataset, similar to the offset reported previously (Laube et al., 2013).

200 The CFC-113 model derived emissions begin in the 1940s and rapidly increase until they peak in 1989 at 251.5 Gg yr^{-1}, then they decrease and in 2016, they are 2.4 Gg yr^{-1} (Figure 4). This sharp decline demonstrates the success of the Montreal Protocol, which came into force in 1989 and phased out the production of CFCs by 1996 in developed countries and 2010 in developing countries (UNEP, 2016a). The total cumulative emissions of CFC-113, up to the end of 2016, are 3163 Gg while the cumulative emissions of CFC-113a are 29 Gg, making the total

205 cumulative emissions of CFC-113a less than 1 % of its isomer CFC-113. Alternatively, in the last decade, 2007-2016, cumulative emissions of CFC-113 are 37 Gg, while for CFC-113a they are 13 Gg, which is about 35 % of the CFC-113 cumulative emissions over this period. This indicates that as emissions of other CFCs are decreasing CFC-113a becomes relatively more important. CFC-113a emissions are now similar to CFC-113 emissions and could become larger in the future if the current trends continue.

210

Up until 1992, the CFC-113 emissions used in the model are the bottom-up emissions estimates from AFEAS. This shows that in the first part of the record, AFEAS reports were accurately reflecting global CFC-113 emissions. However, after 1992 the AFEAS emissions lead to lower modelled mixing ratios than the observations indicating that AFEAS was missing some emissions after 1992. CFC-113 emissions were also derived in another

215 study using a range of emission inventories and estimates (Rigby et al., 2013). These emissions mostly agree with the emissions estimated in this study within the uncertainties, and the differences are likely due to differences in the methods used to calculate the emissions. Rigby et al. (2013) used the estimated emissions to derive the steady-state atmospheric lifetimes whereas in this study, we used the steady-state atmospheric lifetimes to derive the emissions using shorter lifetimes than in Rigby et al. (2013).

220

The upper and lower bounds of the CFC-113 emissions in this study are derived using the 'likely' range in the CFC-113 lifetime given by WMO of 82-109 years (Carpenter and Reimann, 2014). The 'possible' range of 69-138 years was also estimated by Carpenter and Reimann (2014), however with a lifetime of 138 years the modelled mixing ratios did not decrease quickly enough after 1990 to match the downwards trend in CFC-113 observations

225 even with no emissions. This indicates that the maximum possible lifetime of CFC-113 is somewhere between 109 years and 138 years. Setting the emissions to zero from 2003 onwards and adjusting the lifetime so that the model reproduced the CFC-113 mixing ratios at Cape Grim, suggests the maximum lifetime for CFC-113 is 110 years. Combining the measurement and model errors as described in the supplementary material gives an error of 5.7% and applying this to the lifetime gives a maximum lifetime of 110±6 years. For comparison, we also

230 calculated the maximum lifetime from the observed rate of decrease in CFC-113 mixing ratios at Cape Grim between 2003 and 2017 using the continuity equation and assuming no sources of CFC-113 (Supplementary material, Section 2). The agreement was good giving a maximum lifetime of 113±4 years. It should be noted that CFC-113 is not the focus of this study, but we do find that emissions of it persist until 2017, which enables the possibility that some of the recent emissions of CFC-113a are related to CFC-113 emissions, similar to findings

235 for other isomeric CFCs (Laube et al., 2016).

3.2 Global distributions of CFC-113a

3.2.1 Enhancement above background mixing ratios

Many of the CFC-113a mixing ratios at Taiwan (light blue dots, Figure 5) are significantly higher than at the other locations in this study. The background mixing ratios consistently increase through this period from about 0.4 ppt to about 0.7 ppt whereas the highest Taiwan samples have mixing ratios of up to 3 ppt. These large spikes in mixing ratios in all four years of the Taiwan campaigns indicate continued emissions in this region.

These enhancements in CFC-113a mixing ratios are likely due to emissions of this compound in East Asia. To determine the region(s) of origin more accurately NAME footprints are used (Figure 6a-g). In general, the spikes in CFC-113a mixing ratios usually occur when the NAME footprints show that the air most likely came from the boundary layer over eastern China or the Korean peninsula in (a), (c), (d), and (g) for example. Whereas the footprints in (b), (e) and (f) are examples of samples with lower CFC-113a mixing ratios and there is very little influence from eastern China or the Korean peninsula. In (b) and (e), the air is coming from the north, between the eastern coast of China and the Korean peninsula, and in (f) the air mass originates predominantly from over the Pacific Ocean. However, we recognise the limitations of our relatively sparse dataset which prevents us from pinpointing the source region(s) further.

After investigating correlations of CFC-113a with a range of other halocarbons in Taiwan we found CFC-113a mixing ratios correlate well (R^2>0.750) in multiple years with those of CFC-113 and HCFC-133a (CH_2ClCF_3) indicating a possible link between the sources of these compounds (Table 2). CFC-113a correlates well with CFC-113 in 2013 and 2014, but shows almost no correlation in 2015 and a slightly decreased correlation coefficient in 2016 (Table 2, Figure 7). In contrast, HCFC-133a strongly correlates with CFC-113a in all four years (Table 2). HCFC-133a mixing ratios have varied over the last few years. They increased in 2012/2013 and then the trend reversed and in 2014/2015, they decreased (Vollmer et al., 2015). Then according to our latest data from Cape Grim in 2016, they began increasing again. Large changes in emissions are needed to produce this variable trend but it is currently unclear what is causing these changes (Vollmer et al., 2015).

CFC-113a mixing ratios in many of the samples collected from Bachok, Malaysia (grey dots, Figure 5) are also enhanced above background levels although not as much as the Taiwan samples. The mixing ratios range from 0.68 ppt to 1.00 ppt. The higher mixing ratios also have their origin in East Asia being transported rapidly to the tropics by the East Asian winter monsoon circulation (Ashfold et al., 2015; Oram et al., 2017). Figure 8 shows an example NAME footprint from a sample collected in January 2014.

The Tacolneston samples (yellow dots, Figure 5) show no large spikes in CFC-113a mixing ratios. This indicates that Tacolneston is not located close to any sources of CFC-113a and therefore the UK does not have large sources of CFC-113a. Due to this and the relatively long lifetime of CFC-113a Tacolneston can be considered to be representative of Northern Hemisphere background mixing ratios of CFC-113a. Both sites in Taiwan and also Tacolneston are Northern Hemisphere sites and although the Taiwan sites have large spikes in CFC-113a mixing ratios there are some samples with background mixing ratios. For example, in spring 2016, the only period for which these datasets overlap, the lowest CFC-113a mixing ratio in Taiwan is 0.70 ppt on 24/03/16 (Figure 6e). The closest Tacolneston sample to this is on 04/04/16 with a CFC-113a mixing ratio of 0.71 ppt. This shows that Taiwan can encounter mixing ratios at background levels of CFC-113a. However, many of the air samples collected in Taiwan show mixing ratios of CFC-113a above background levels, suggesting that enhanced levels of CFC-113a are generally widespread across this region.

3.2.2 Interhemispheric gradient of CFC-113a

For the period when measurements were made at both Cape Grim and Tacolneston (from July 2015 to February 2017), the Tacolneston mixing ratios were generally higher than the Cape Grim mixing ratios (Figure 5-inset). On average Cape Grim mixing ratios are 0.055 ± 0.024 ppt higher than Tacolneston mixing ratios. This shows that there is an interhemispheric gradient with higher CFC-113a mixing ratios in the Northern Hemisphere as would be expected for a compound emitted primarily in the Northern Hemisphere. This interhemispheric gradient is further supported by the six CARIBIC flights from Germany to South Africa between 2009 and 2016. The CARIBIC samples (purple dots) from the 2016 flight coincide temporally with the Tacolneston and the Cape Grim samples in Fig. 5 and confirm the observation of higher mixing ratios in the Northern Hemisphere (filled purple

285 dots) and lower mixing ratios in the Southern Hemisphere (unfilled purple dots). Also see Fig. S1a in the supplementary material.

Laube et al. (2014) also found an interhemispheric gradient in CFC-113a using four of these CARIBIC flights 2009-2011 and furthermore they found that the increasing trend of CFC-113a at Cape Grim, lagged behind the increasing trend inferred from the firn air samples from Greenland, in the Northern Hemisphere. As the firn air

290 measurements in the Laube et al. (2014) study were collected in Greenland between 14-30 July 2008, the surface measurements will be representative of atmospheric mixing ratios at that time. They will also be representative of background Northern Hemispheric CFC-113a mixing ratios as the Greenland firn air location was isolated from any large industrial areas with potential sources of CFC-113a. Figure 5 includes the three measurements closest to the surface (brown dots) although they are so close together that they appear to be one dot in the figure and the

295 average mixing ratio of the three samples is 0.44 ± 0.01 ppt.

Overall, these measurements demonstrate that there is an interhemispheric gradient in CFC-113a with higher mixing ratios in the Northern Hemisphere. This persistent interhemispheric difference indicates ongoing emissions of CFC-113a in the Northern Hemisphere or higher emissions in the Northern Hemisphere compared to the Southern Hemisphere. Similar interhemispheric gradients have been found for other CFCs (Liang et al.,

300 2008), as CFCs are almost exclusively produced by industrial processes and most industrial production (and consumption) takes place in the Northern Hemisphere.

3.2.3 Measurements of CFC-113a in the stratosphere

Air samples are usually collected on the CARIBIC flights at cruising altitudes of 10-12 km, which for samples over northern India, during four flights going from Germany to Thailand (green dots, Figure 5) would be at the

305 tropopause. The measurements should thus be representative of the mixing ratios of compounds just prior to entering the tropical tropopause layer (TTL) which is the main entrance region to the stratosphere (Fueglistaler et al., 2009). For the flight on 9/11/2013, there is some enhancement above background mixing ratios over South-East Asia (Figures 5, S1b). This is likely due to air being transported from East Asia into the tropics via cold surges and then being transported up into the upper troposphere via convection (Oram et al., 2017). This means

310 that the uplift mechanism in this region could potentially enhance concentrations of long-lived ODSs entering the stratosphere as compared to the 'background' clean air ground-based abundances that are normally used to derive such inputs (Carpenter and Reimann, 2014).

The Geophysica flights reach altitudes of 20 km and so take samples of stratospheric air. The Geophysica 2009-2010 flights (pink dots) and the Geophysica 2016 flights (orange dots) begin at background mixing ratios and then

315 decrease (Figure 5). During the 2016 flights, for example, measurements start at 10 km altitude where mixing ratios are 0.71 ppt and go up to 20 km where the mixing ratios are 0.36 ppt. In comparison to this, ground level measurements made at the Northern Hemisphere site, Tacolneston, had an average CFC-113a mixing ratio in 2016 of 0.72 ppt. In general, mixing ratios decrease as the aircraft ascends. This is because air at higher altitudes will have taken longer to travel there and therefore is older and CFC-113a at higher altitudes has experienced photolytic

320 decomposition. For more information about the Geophysica flights see the supplementary material.

4. Possible sources of CFC-113a

CFCs are entirely anthropogenic in origin. It is therefore likely that there is a continuing industrial process(es) either producing or involving CFC-113a that leads to continuing emissions of substantial amounts of this compound into the atmosphere, especially in East Asia. Whilst the Montreal Protocol has banned the production

325 and consumption of CFCs, there are exemptions including the use of ODSs as chemical feedstocks. Whilst feedstock usage has to be reported to the United Nations Environment Programme (UNEP), these data are not publicly available (UNEP, 2016a). Also the Montreal Protocol does not require isomers to be reported separately, so CFC-113 and CFC-113a may be reported together. Furthermore, the use of ODSs as intermediate species and trace amounts of fugitive emissions do not have to be reported. Therefore, possible sources for the increase in

330 CFC-113a mixing ratios include its use as a chemical feedstock, chemical intermediates, and fugitive emissions as well as unsanctioned production (Laube et al., 2014).

The strong correlations of CFC-113a with CFC-113 and HCFC-133a in Taiwan (Section 3.2.1) suggest that they are involved in the same production pathways or that their production facilities are co-located. The absence of a correlation between CFC-113a and CFC-113 in 2015 in Taiwan is not what we would expect based on their source type (industry) and lifetimes. In addition, the overall mixing ratios in 2015 appear to be lower than in the other years and have fewer large spikes (Figure 7). This could be because in general less air was arriving from China/Korea in 2015, which is indicated by the NAME footprints (Supplementary material, Section 5). China/Korea were the areas we found to be the most likely source of CFC-113a emissions. Alternatively, the varying correlations in different years between CFC-113a and CFC-113 could indicate that there is more than one process emitting CFC-113a in East Asia, or variability in the process or in the amount of leaking of gases. This may be an indication of two or more independent sources of CFC-113a. CFC-113 feedstock use decreased by over 50% in 2015 due to one producer, which is also a user choosing not to produce CFC-113 in 2015 and reducing in-house inventories instead (Maranion et al., 2017). If this were the process leading to correlated emissions of CFC-113a and CFC-113 this may explain their lack of correlation in 2015.

One possible source of CFC-113a is from HFC production, specifically, of HFC-134a (CH$_2$FCF$_3$) and HFC-125 (CF$_3$CHF$_2$), as both involve CFC-113a in their production process. There are two main routes for making HFC-134a (Manzer, 1990). The first begins with CFC-113 being isomerised to form CFC-113a, which is then fluorinated to produce CFC-114a (CF$_3$CCl$_2$F), the latter is then hydrogenated to produce HFC-134a (Manzer, 1990). The other production method involves the reaction of hydrogen fluoride with trichloroethylene to form HCFC-133a and HFC-134a (Manzer, 1990). The process for manufacturing HFC-125 involves the starting materials of either HCFC-123 or HCFC-124. CFC-113a, CFC-113 and HCFC-133a can be formed as by-products when HCFC-123 and HCFC-124 are fluorinated and recycled during the process that forms HFC-125 (Kono et al., 2002).

If there were any leaks in the system or venting of gases during these processes, this could lead to enhanced mixing ratios of CFC-113a and strong correlations with its isomer CFC-113 and HCFC-133a. HFC production should be contained and involve no fugitive emissions to the atmosphere. However, the Chemicals Technical Options Committee (CTOC) 2014 report suggests there may be small leaks, depending on the quality of the system, ranging between 0.1 % and 5 % of the feedstock used. The CTOC reported that a leak rate of about 1.6 % would be needed if all CFC-113a and HCFC-133a in the atmosphere had come from their use as feedstock in the production of HFC-134a, HFC-125 and HFC-143a, which is within the previous range (CTOC, 2014). HFC-143a is produced using HCFC-133a so it was included in the CTOC estimate but CFC-113a is not involved in its production so it is not included in this study (CTOC, 2014).

Observed HFC-134a and HFC-125 mixing ratios are not well correlated with those of CFC-113a, CFC-113 or HCFC-133a, except for HFC-125 in 2016 that has a good correlation with CFC-113a (Table 2). We would not necessarily expect them to be well correlated as most of the emissions of the HFCs are usually related to their uses rather than their production. For example, as HFC-134a is used in mobile air conditioning units and in refrigeration, we would expect a significant component of HFC-134a emissions to be related to automobile use. CFC-114a is also part of the production process of HFC-134a (Manzer, 1990), and can be another by-product during HFC-125 production (Kono et al., 2002). CFC-114a was only measured in 2015 and 2016 in Taiwan and was strongly correlated with CFC-113a in 2015 but not in 2016. This inconsistent correlation does not help to define further the source of CFC-113a. Furthermore HCFC-123 mixing ratios are not well correlated with CFC-113a, CFC-113 or HCFC-133a in any year in Taiwan but HCFC-124 mixing ratios are well correlated in 2015 with CFC-113a (Table 2) and with HCFC-133a (R^2=0.791). This strong correlation with HCFC-124 points to HFC-125 production being the dominant source in 2015.

On the one hand, the Cape Grim dataset shows that CFC-113a and CFC-113 have very different atmospheric trends (Figures 3, 4) but on the other hand, the Taiwan dataset shows that the isomers are mostly strongly correlated (Figure 7). This is not necessarily a contradiction because, close to sources the two compounds would still be correlated, but the emissions are low in absolute numbers for CFC-113 so it is globally still decreasing. In Sect. 3.1 we concluded that there was possibly a small amount of continued emissions of CFC-113 to maintain

380   the observed atmospheric mixing ratios. This would be consistent with either a source from banks and/or release in conjunction with CFC-113a.

As discussed above, eastern China or the Korean peninsula are the most likely sources of the elevated mixing ratios of CFC-113a observed in Taiwan, and the HFC industry in China has been growing rapidly in recent years (Fang et al., 2016). In China in 2013, productions of 118 Gg yr^{-1} of HFC-134a and 78 Gg yr^{-1} of HFC-125 were

385   reported (Fang et al., 2016). Most industry in China is located on the eastern coast and the majority of HFC manufacturers are in the three eastern provinces of Shanghai, Zhejiang and Jiangsu. There are also HFC-134a and HFC-125 production plants in Japan, South Korea and Taiwan but the majority are located in China. The HFC production plants located in Taiwan could influence the mixing ratios at both the sites in Taiwan and as we do not know where they are located, this introduces an additional uncertainty. We suggest that the CFC-113a emissions

390   in the atmosphere originate predominantly from HFC production; however, there is currently insufficient data available to conclude this with high confidence.

Alternatively, there is an official exemption in the Montreal Protocol for the use of CFC-113a as an "agrochemical intermediate for the manufacture of synthetic pyrethroids", (UNEP, 2003) probably because it is used to make the insecticides cyhalothrin and tefluthrin (Brown et al., 1994). CFC-113 is a feedstock used to make trifluoroacetic

395   acid (TFA) and pesticides (Maranion et al., 2017). In addition CFC-113a is an intermediate in this process and these production processes are used in India and China and so this could also be a source in this region (Maranion et al., 2017). Furthermore HCFC-133a is also used to manufacture TFA and agrochemicals although the process involving HCFC-133a is not related to the process involving CFC-113a (Rüdiger et al., 2002; Maranion et al., 2017).

400   Furthermore, CFC-113a is potentially present as an impurity in CFC-113 and the emissions of CFC-113a could be from CFC-113 banks. We saw in Sect. 3.2 that estimated emissions of CFC-113a began in the 1960s and HFC production did not become a large-scale industry until much later, so there must have been another source of CFC-113a during that earlier part of the record.

To summarise we have identified four possible sources of CFC-113a: agrochemical production, HFC-134a

405   production, HFC-125 production and an impurity in CFC-113. The correlations indicate that HFC production is the dominant source in the East Asian region. Overall, the sources of CFC-113a emissions are still uncertain and further evidence is needed to quantify and pinpoint them. However, the likely sources we have found do not necessarily indicate a breach of the treaty as the use of CFCs as intermediates in the production of other compounds are permitted under the Montreal Protocol.

410   **5. Conclusions**

There is a continued global increasing trend in CFC-113a mixing ratios based on a number of globally distributed sampling activities giving a consistent picture. CFC-113a mixing ratios at Cape Grim, Australia increased since the previous study from 0.50 ppt in December 2012 to 0.70 ppt in February 2017. The derived emissions were still significantly above 2010 levels and were on average 1.7 Gg yr^{-1} (1.3-2.4 Gg yr^{-1}) between 2012 and 2016.

415   Additionally, CFC-113a mixing ratios vary globally and our findings confirm an interhemispheric gradient with mixing ratios decreasing from the Northern Hemisphere to the Southern Hemisphere. No significant emissions of CFC-113a occur in the UK but strong sources exist in East Asia. There are multiple possible sources of CFC-113a emissions and correlation analysis suggests the emissions might be associated with the production of HFC-134a and HFC-125.

420   The background abundances of CFC-113a reported here are currently small (<1.0 ppt) in comparison to the most common CFC, CFC-12 which has atmospheric mixing ratios of ~510 ppt in 2017 (NOAA, 2017). Therefore, the contribution of CFC-113a to stratospheric ozone depletion is comparably small and is not yet a cause for major concern. While its increase in recent years has been considerable in percentage terms, it would have to continue increasing at this rate for several centuries before it reaches the atmospheric mixing ratios of the major CFCs in

425   the 1990s. In 2016, HFCs were added to the Montreal Protocol and under the new amendment HFC consumption will be phased down in the coming decades (UNEP, 2016b). Therefore, if this phase down schedule is successful

and the main source of CFC-113a is indeed from HFC production, then CFC-113a atmospheric mixing ratios should stop increasing in the future. However, whilst it seems likely, it is still not clear whether HFC production is actually the main source of global CFC-113a emissions. Further investigation and continued monitoring is
430 needed to assess future changes and ensure the continued effectiveness of the Montreal Protocol. What is required is continuous measurements of CFC-113a in the East Asia region. With such data the magnitude and origins of East Asian CFC-113a emissions could be quantified.

In the past, it was assumed that isomers of CFCs had similar uses, sources and trends and therefore it was not necessary to report them separately. However, in this study, we have found that the isomers CFC-113a and CFC-
435 113 continue to have different trends in the atmosphere and in their emissions. Recently CFC-114a (CF_3CCl_2F) and CFC-114 ($CClF_2CClF_2$) were also found to have different trends and sources (Laube et al., 2016). Therefore, we recommend that atmospheric observational data on individual CFC isomers be reported to UNEP wherever possible. In addition, the increase in CFC-113a demonstrates that ODSs used as chemical feedstock or intermediates might need to start being regulated by the Montreal Protocol as the use of ODSs for direct
440 applications decreases, the use of ODSs as chemical feedstock or intermediates is becoming relatively more important.

6. Data availability

All data have been made publicly available in the supplement.

Competing interests. The authors declare that they have no conflict of interest.

445 **Acknowledgements**

We are grateful for the work of the Geophysica team, the CARIBIC team, the staff at the Cape Grim station, the NOAA Global Monitoring Division, and the AGAGE network. The StratoClim flights were funded by the European Commission (FP7 project Stratoclim-603557, www.stratoclim.org). The collection and curation of the Cape Grim Air Archive is jointly funded by CSIRO, the Bureau of Meteorology (BoM) and Refrigerant Reclaim
450 Australia.; BoM/CGBAPS staff at Cape Grim were/are largely responsible for the collection of archive samples and UEA flask air samples; the original (mid-1990s) subsampling of the archive for UEA was funded by AFEAS and CSIRO, ongoing subsampling by CSIRO. K. E. Adcock was supported by the UK Natural Environment Research Council (PhD studentship NE/L002582/1). J. C. Laube received funding from the UK Natural Environment Research Council (Research Fellowship NE/I021918/1). Norfazrin Mohd Hanif has been funded
455 through PhD studentship by the Ministry of Education Malaysia (MOE) and Universiti Kebangsaan Malaysia (UKM). We acknowledge use of the NAME atmospheric dispersion model and associated NWP meteorological data sets made available to us by the UK Met Office. We also acknowledge the significant storage resources and analysis facilities made available to us on JASMIN by STFC CEDA along with the corresponding support teams.

References

460 Ashfold, M. J., Pyle, J. A., Robinson, A. D., Meneguz, E., Nadzir, M., Phang, S. M., Samah, A. A., Ong, S., Ung, H. E., Peng, L. K., Yong, S. E., Harris, N. R. P. and Ashfold, M.: Rapid transport of East Asian pollution to the deep tropics, Atmos. Chem. Phys, 15, 3565–3573, doi:10.5194/acp-15-3565-2015, 2015.

Brenninkmeijer, C. A. M., Crutzen, P., Boumard, F., Dauer, T., Dix, B., Ebinghaus, R., Filippi, D., Fischer, H., Franke, H., Frieß, U., Heintzenberg, J., Helleis, F., Hermann, M., Kock, H. H., Koeppel, C., Lelieveld, J.,
465 Leuenberger, M., Martinsson, B. G., Miemczyk, S., Moret, H. P., Nguyen, H. N., Nyfeler, P., Oram, D., O'sullivan, D., Penkett, S., Platt, U., Pupek, M., Ramonet, M., Randa, B., Reichelt, M., Rhee, T. S., Rohwer, J., Rosenfeld, K., Scharffe, D., Schlager, H., Schumann, U., Slemr, F., Sprung, D., Stock, P., Thaler, R., Valentino, F., Van Velthoven, P., Waibel, A., Wandel, A., Waschitschek, K., Wiedensohler, A., Xueref-Remy, I., Zahn, A., Zech, U. and Ziereis, H.: Civil Aircraft for the regular investigation of the atmosphere based on an instrumented
470 container: The new CARIBIC system, Atmos. Chem. Phys., 7, 4953–4976, doi:10.5194/acp-7-4953-2007, 2007.

Brown, S. M., Glass, J. C. and Sheldrake, G. N.: Preparation of 1,1,1,trichlorotrifluoroethane, UK Patent Application, GB2269381A, [online] Available from:
https://patents.google.com/patent/GB2269381A/en?q=%22CFC-

475   113a%22,trichlorotrifluoroethane,CCl3CF3&q=cyhalothrin,Lambda-
       cyhalothrin,C23H19ClF3NO3&q=tefluthrin,C17H14ClF7O2&q=C07C17%2F10, 1994.

       Buizert, C., Martinerie, P., Petrenko, V. V., Severinghaus, J. P., Trudinger, C. M., Witrant, E., Rosen, J. L.,
       Orsi, A. J., Rubino, M., Etheridge, D. M., Steele, L. P., Hogan, C., Laube, J. C., Sturges, W. T., Levchenko, V.
       A., Smith, A. M., Levin, I., Conway, T. J., Dlugokencky, E. J., Lang, P. M., Kawamura, K., Jenk, T. M., White,
       J. W. C., Sowers, T., Schwander, J. and Blunier, T.: Gas transport in firn: Multiple-tracer characterisation and
480   model intercomparison for NEEM, Northern Greenland, Atmos. Chem. Phys., 12, 4259–4277, doi:10.5194/acp-
       12-4259-2012, 2012.

       Carpenter, L. J., Reimann, S. (Lead Authors), Burkholder, J. B., Clerbaux, C., Hall, B. D., Hossaini, R., Laube,
       J. C. and Yvon-Lewis, S. A.: Chapter 1: Update on Ozone-Depleting Substances (ODSs) and Other Gases of
       Interest to the Montreal Protocol, in Scientific Assessment of Ozone Depletion: 2014, Global Ozone Research
485   and Monitoring Project – Report No. 55, World Meteorological Organization, Geneva, Switzerland., 2014.

       Chemicals Technical Options Committee (CTOC): Montreal Protocol on Substances that Deplete the Ozone
       Layer Report of the Chemicals Technical Options Committee 2014 Assessment Report. [online] Available from:
       http://ozone.unep.org/Assessment_Panels/TEAP/Reports/CTOC/, 2014.

       Fang, X., Velders, G. J. M., Ravishankara, A. R., Molina, M. J., Hu, J. and Prinn, R. G.: Hydrofluorocarbon
490   (HFC) Emissions in China: An Inventory for 2005-2013 and Projections to 2050, Environ. Sci. Technol., 50(4),
       2027–2034, doi:10.1021/acs.est.5b04376, 2016.

       Farman, J. C., Gardiner, B. G. and Shanklin, J. D.: Large losses of total ozone in Antarctica reveal seasonal
       ClOx/NOx interaction, Nature, 315, 207–210, doi:10.1038/315207a0, 1985.

       Fraser, P., Oram, D., Reeves, C., Penkett, S. and McCulloch, A.: Southern Hemisphere halon trends (1978-
495   1998) and global halon emissions, J. Geophys. Res, 104(D13), 15985–15999, doi:10.1029/1999JD900113,
       1999.

       Fueglistaler, S., Dessler, A. E., Dunkerton, T. J., Folkins, I., Fu, Q. and Mote, P. W.: Tropical Tropopause
       Layer, Rev. Geophys., 47, RG1004, doi:10.1029/2008RG000267, 2009.

       Ganesan, A. L., Manning, A. J., Grant, A., Young, D., Oram, D. E., Sturges, W. T., Moncrieff, J. B. and O
500   'Doherty, S.: Quantifying methane and nitrous oxide emissions from the UK and Ireland using a national-scale
       monitoring network, Atmos. Chem. Phys, 15, 6393–6406, doi:10.5194/acp-15-6393-2015, 2015.

       Jones, A., Thomson, D., Hort, M. and Devenish, B.: The U.K. Met Office's Next-Generation Atmospheric
       Dispersion Model, NAME III, in Air Pollution Modeling and Its Application XVII, edited by C. Borrego and
       A.-L. Norman, pp. 580–589, Springer US., 2007.

505   Kaiser, J., Engel, A., Borchers, R. and Röckmann, T.: Probing stratospheric transport and chemistry with new
       balloon and aircraft observations of the meridional and vertical N2O isotope distribution, Atmos. Chem. Phys.,
       6(11), 3535–3556, doi:10.5194/acp-6-3535-2006, 2006.

       Kono, S., Yoshimura, T. and Shibanuma, T.: Process for producing 1,1,1,2,2-pentafluoroethane, United States
       Patent, US Patent 6,392,106 B1, [online] Available from:
510   https://patentimages.storage.googleapis.com/96/18/bb/1942c2e2d57286/US6392106.pdf (Accessed 5 September
       2017), 2002.

       Laube, J. C., Martinerie, P., Witrant, E., Blunier, T., Schwander, J., Brenninkmeijer, C. A. M., Schuck, T. J.,
       Bolder, M., Röckmann, T., Van Der Veen, C., Bönisch, H., Engel, A., Mills, G. P., Newland, M. J., Oram, D.
       E., Reeves, C. E. and Sturges, W. T.: Accelerating growth of HFC-227ea (1,1,1,2,3,3,3- heptafluoropropane) in
515   the atmosphere, Atmos. Chem. Phys., 10(13), 5903–5910, doi:10.5194/acp-10-5903-2010, 2010.

       Laube, J. C., Hogan, C., Newland, M. J., Mani, F. S., Fraser, P. J., Brenninkmeijer, C. A. M., Martinerie, P.,
       Oram, D. E., Röckmann, T., Schwander, J., Witrant, E., Mills, G. P., Reeves, C. E. and Sturges, W. T.:
       Distributions, long term trends and emissions of four perfluorocarbons in remote parts of the atmosphere and
       firn air, Atmos. Chem. Phys., 12(9), 4081–4090, doi:10.5194/acp-12-4081-2012, 2012.

520   Laube, J. C., Keil, A., Bönisch, H., Engel, A., Röckmann, T., Volk, C. M. and Sturges, W. T.: Observation-
       based assessment of stratospheric fractional release, lifetimes, and ozone depletion potentials of ten important

source gases, Atmos. Chem. Phys, 13, 2779–2791, doi:10.5194/acp-13-2779-2013, 2013.

Laube, J. C., Newland, M. J., Hogan, C., Brenninkmeijer, C. a. M., Fraser, P. J., Martinerie, P., Oram, D. E., Reeves, C. E., Röckmann, T., Schwander, J., Witrant, E. and Sturges, W. T.: Newly detected ozone-depleting
525   substances in the atmosphere, Nat. Geosci., 7(March), 10–13, doi:10.1038/NGEO2109, 2014.

Laube, J. C., Hanif, N. M., Martinerie, P., Gallacher, E., Fraser, P. J., Langenfelds, R., Brenninkmeijer, C. A. M., Schwander, J., Witrant, E., Wang, J.-L., Ou-Yang, C.-F., Gooch, L. J., Reeves, C. E., Sturges, W. T. and Oram, D. E.: Tropospheric observations of CFC-114 and CFC-114a with a focus on long-term trends and emissions, Atmos. Chem. Phys, 16, 15347–15358, doi:10.5194/acp-16-15347-2016, 2016.

530   Liang, Q., Stolarski, R. S., Douglass, A. R., Newman, P. A. and Nielsen, J. E.: Evaluation of emissions and transport of CFCs using surface observations and their seasonal cycles and the GEOS CCM simulation with emissions-based forcing, J. Geophys. Res. Atmos., 113(14), 1–15, doi:10.1029/2007JD009617, 2008.

Manzer, E. L.: The CFC-Ozone Issue: Progress on the Development of Alternatives to CFCs, Science, 249(4964), 31–35, doi:10.1126/science.249.4964.31, 1990.

535   Maranion, B., Pizano, M. and Woodcock, A.: Montreal Protocol on Substances that Deplete the Ozone Layer, Report of the UNEP Technology and Economic Assessment Panel, Volume 1, Progress Report, May 2017, Nairobi, Kenya. [online] Available from: http://conf.montreal-protocol.org/meeting/oewg/oewg-39/presession/Background-Documents/TEAP-Progress-Report-May2017.pdf (Accessed 19 September 2017), 2017.

540   McCulloch, A., Midgley, P. M. and Fisher, D. A.: Distribution of emissions of chlorofluorocarbons (CFCs) 11, 12, 113, 114 and 115 among reporting and non-reporting countries in 1986, Atmos. Environ., 28(16), 2567–2582, doi:10.1016/1352-2310(94)90431-6, 1994.

Molina, M. J. and Rowland, F. S.: Stratospheric sink for chlorofluoromethanes: chlorine atom-catalysed destruction of ozone, Nature, 249, 810–812, doi:10.1038/249810a0, 1974.

545   Montzka, S. A., Bulter, J. H., Elkins, J. W., Thompson, T. M., Clarke, A. D. and Lock, L. T.: Present and future trends in the atmospheric burden of ozone-depleting halogens, Nature, 398, 690–694, 1999.

Montzka, S. A., Hall, B. D. and Elkins, J. W.: Accelerated increases observed for hydrochlorofluorocarbons since 2004 in the global atmosphere, Geophys. Res. Lett., 36(3), 1–5, doi:10.1029/2008GL036475, 2009.

National Oceanic and Atmospheric Administration (NOAA): GMD Data Archive, [online] Available from:
550   ftp://ftp.cmdl.noaa.gov/hats/cfcs/cfc12/combined/HATS_global_F12.txt (Accessed 24 April 2017), 2017.

Newland, M. J., Reeves, C. E., Oram, D. E., Laube, J. C., Sturges, W. T., Hogan, C., Begley, P. and Fraser, P. J.: Southern hemispheric halon trends and global halon emissions, 1978-2011, Atmos. Chem. Phys., 13(11), 5551–5565, doi:10.5194/acp-13-5551-2013, 2013.

Oram, D. E., Ashfold, M. J., Laube, J. C., Gooch, L. J., Humphrey, S., Sturges, W. T., Leedham-Elvidge, E.,
555   Forster, G. L., Harris, N. R. P., Mead, M. I., Samah, A. A., Phang, S. M., Ou-Yang, C.-F., Lin, N.-H., Wang, J.-L., Baker, A. K., Brenninkmeijer, C. A. M. and Sherry, D.: A growing threat to the ozone layer from short-lived anthropogenic chlorocarbons, Atmos. Chem. Phys, 175194, 11929–11941, doi:10.5194/acp-17-11929-2017, 2017.

Pawson, S., Steinbrecht, W. (Lead Authors), Charlton-Perez, A. J., Fujiwara, M., Karpechko, A. Y.,
560   Petropavlovskikh, I., Urban, J. and Weber, M.: Chapter 2: Update on global ozone: Past, present, and future, in Scientific Assessment of Ozone Depletion: 2014, Global Ozone Research and Monitoring Project – Report No. 55, World Meteorological Organization, Geneva, Switzerland., 2014.

Reeves, C. E., Sturges, W. T., Sturrock, G. A., Preston, K., Oram, D. E., Schwander, J., Mulvaney, R., Barnola, J.-M. and Chappellaz, J.: Trends of halon gases in polar firn air: implications for their emission distributions,
565   Atmos. Chem. Phys, 5, 2055–2064, doi:10.5194/acp-5-2055-2005, 2005.

Rigby, M., Prinn, R. G., Montzka, S. A., McCulloch, A., Harth, C. M., Uhle, J., Salameh, P. K., Weiss, R. F., Young, D., Simmonds, P. G., Hall, B. D., Dutton, G. S., Nance, D., Mondeel, D. J., Elkins, J. W., Krummel, P. B., Steele, L. P. and Fraser, P. J.: Re-evaluation of the lifetimes of the major CFCs and CH_3CCl_3 using

atmospheric trends, Atmos. Chem. Phys, 13, 2691–2702, doi:10.5194/acp-13-2691-2013, 2013.

570   Rüdiger, S., Gross, U., Shekar, S. C., Rao, V. V., Sateesh, M. and Kemnitz, E.: Studies on the conversion of
      1,1,1-trichlorotrifluoroethane, chloro-2,2,2-trifluoroethane, and 1,1,1-trifluoroethane by catalytic oxidation,
      hydrolysis and ammonolysis, Green Chem., 4(6), 541–545, doi:10.1039/B206098C, 2002.

      Solomon, S., Ivy, D. J., Kinnson, D., Mills, M. J., Neely III, R. R. and Schmidt, A.: Emergence of healing in the
      Antarctic ozone layer, Science, 353(6296), 269–274, doi:10.1126/science.aae0061, 2016.

575   United Nations Environment Programme (UNEP): Fifteenth Meeting of the Parties to the Montreal Protocol on
      Substances that Deplete the Ozone Layer, Nairobi, 10-14 November 2003, New Ozone-Depleting Substances
      that have been Reported by the Parties, UNEP/OzL.Pro.15/INF/2, [online] Available from:
      http://www.42functions.eu/new_site/en/meetings/mop/mop15-index.php (Accessed 18 October 2017), 2003.

      United Nations Environment Programme (UNEP): Twenty-Eighth Meeting of the Parties to the Montreal
580   Protocol on Substances that Deplete the Ozone Layer, Kigali, 10–14 October 2016, Decision XXVIII/1 Further
      Amendment of the Montreal Protocol. [online] Available from:
      http://ozone.unep.org/sites/ozone/files/Publications/Handbooks/Montreal-Protocol-English.pdf (Accessed 21
      July 2017), 2016a.

      United Nations Environment Programme (UNEP): Amendment to the Montreal Protocol on Substances that
585   Deplete the Ozone Layer Decision XXVII/1, UNEP/OzL.Pro.28/CRP/10. [online] Available from:
      http://conf.montreal-protocol.org/meeting/mop/mop-28/final-report/English/Kigali_Amendment-English.pdf
      (Accessed 18 July 2017), 2016b.

      Vollmer, M. K., Rigby, M., Laube, J. C., Henne, S., Siek, T., Gooch, L. J., Wenger, A., Young, D., Steele, L. P.,
      Langenfelds, L., Brenninkmeijer, C. A. M., Wang, J., Wyss, S. A., Hill, M., Oram, D. E., Krummel, P. B.,
590   Schoenenberger, F., Zellweger, C., Fraser, P. J., William, T., Doherty, S. O. and Reimann, S.: Abrupt reversal of
      HCFC-133a (CF$_3$CH$_2$Cl) in the atmosphere, Geophys. Res. Lett., 1–9, doi:10.1002/2015GL065846, 2015.
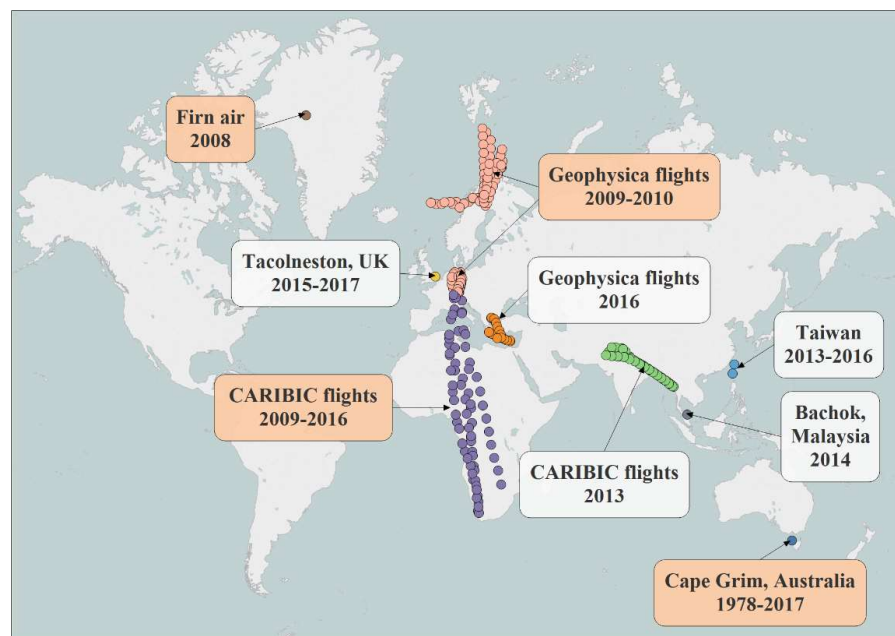
Figure 1. Sampling locations used in this study. Those locations that have been added since Laube et al. (2014) are in white. Those shaded orange featured in, or have been extended since, the Laube et al. paper.

595

Table 1. Air sampling campaigns from which atmospheric CFC-113a mixing ratios were measured, including the data published in Laube et al. (2014).

Sampling campaign	Location	Longitude and Latitude	Dates	No. of samples	Nature of data
NEEM	Greenland	77.445° N, 51.066° W 2484m a.s.l.	14/07/2008– 30/07/2008	3 closest to the surface	Firn air surface data
Cape Grim	Tasmania, Australia	40.683° S, 144.690° E	(07/07/1978) 14/03/2013– 23/02/2017	66 in total, 20 new	Southern Hemisphere ground-based site
Taiwan	East Asia	Hengchun, 22.0547° N, 120.6995° E, (2013, 2015) Cape Fuguei, 25.297° N, 121.538° E, (2014, 2016)	2013–2016	2013: 19 2014: 23 2015: 23 2016: 33	Northern Hemisphere ground-based sites
Tacolneston Tower	Norfolk, United Kingdom	52.3104° N, 1.0820° E	13/07/2015– 16/03/2017	47	Northern Hemisphere tall tower site
Bachok Marine Research Station	Bachok, Malaysia	6.009° N, 102.425° E	20/01/2014– 03/02/2014	16	Tropical ground-based site
Geophysica flights 2009-2010	North Sea	76-48° N, 28-0° E	30/10/2009– 02/02/2010	98	Research aircraft
Geophysica flights 2016	Mediterranean Sea	33-41° N, 22-32° E	01/09/2016 06/09/2016	23	Research aircraft
CARIBIC flights	Germany to South Africa	48° N-30° S, 6-19° E	27/10/2009 28/10/2009 14/11/2010 20/03/2011 10/02/2015 13/01/2016	14 7 13 14 15 7	Commercial aircraft
CARIBIC flights	Germany to Thailand	32-17° N, 70-97° E	21/02/2013 21/03/2013 09/11/2013 05/12/2013	14 7 14 14	Commercial aircraft
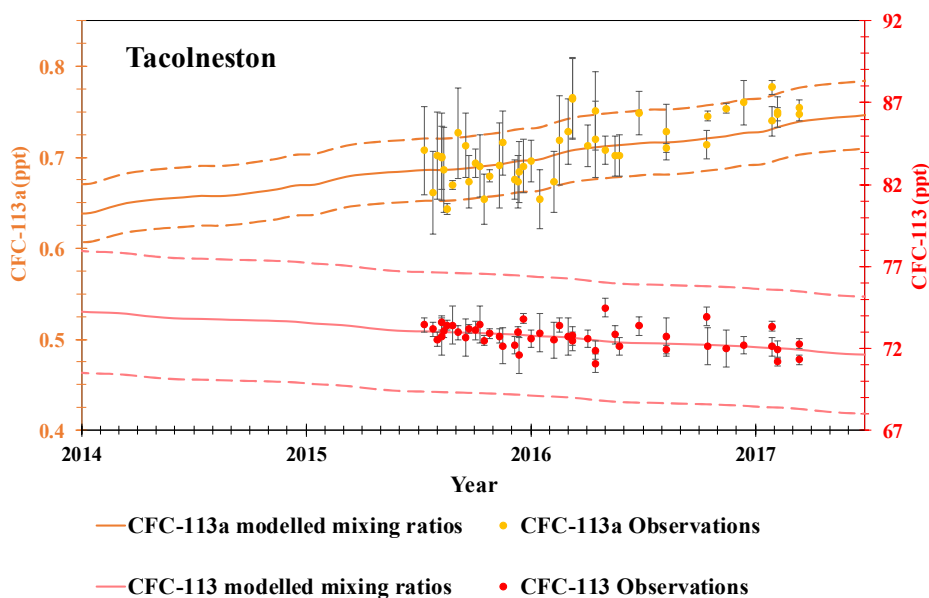
Figure 2. CFC-113a and CFC-113 modelled and observed mixing ratios at Tacolneston. The error bars represent
the 1σ standard deviation. The modelled uncertainties are 5% and are based on the model reproducing the
reported mixing ratios of CFC-11 and CFC-12 at Cape Grim to within 5 % uncertainty (Reeves et al., 2005).
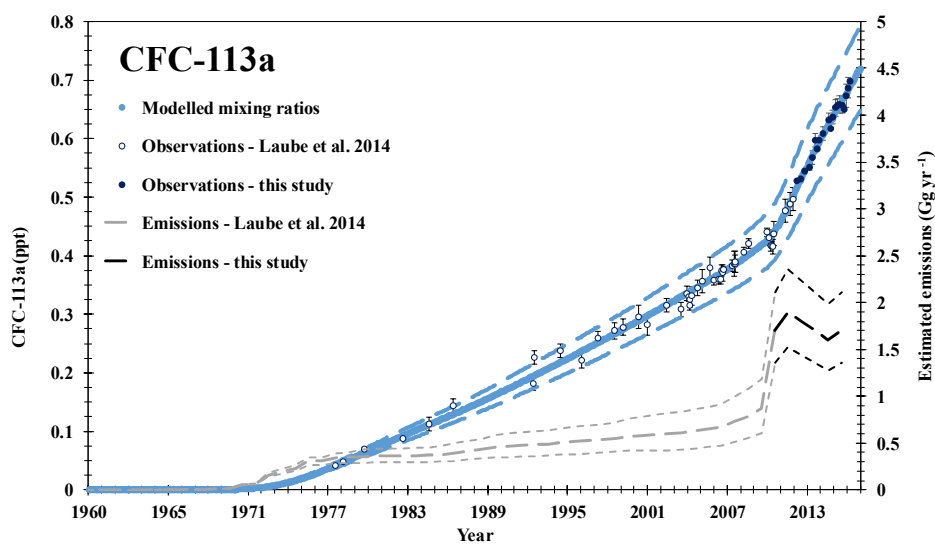
Figure 3. CFC-113a modelled and observed mixing ratios at Cape Grim 1960-2017 and estimated global annual
emissions of CFC-113a. The observations are from July 1978-February 2017 with 1σ standard deviations as error
bars. Data prior to 04/12/2012 is from Laube et al. (2014). The dashed black and grey lines represent the modelled
'best fit' emissions with uncertainties (short-dashed). The method used for calculating the upper and lower
emission bounds is in the supplementary material.
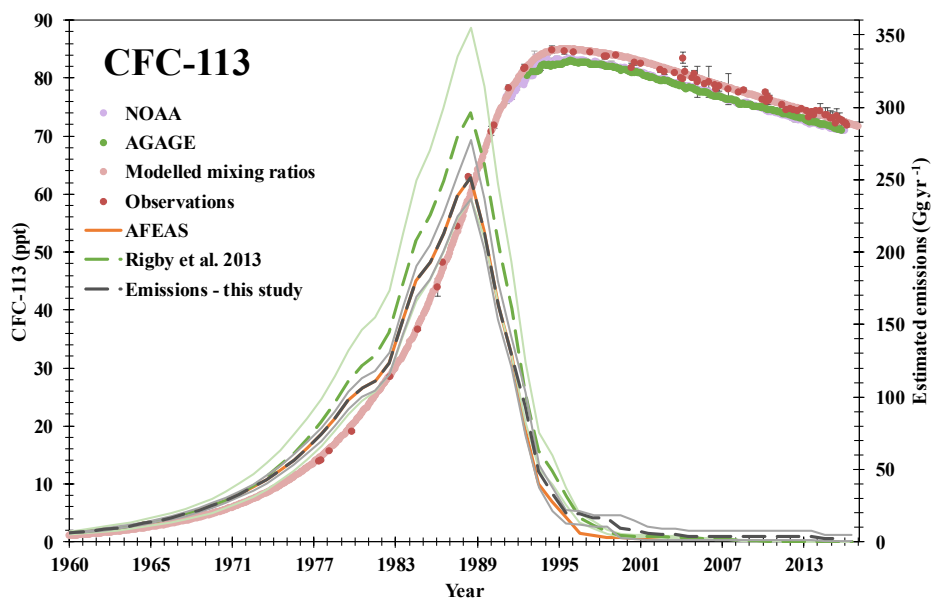
610 Figure 4. CFC-113 modelled and observed mixing ratios at Cape Grim 1960-2017 and estimated global annual emissions of CFC-113. The observations are from Cape Grim, Tasmania, July 1978-February 2017 with 1σ standard deviations as error bars. Also for comparison are the NOAA and AGAGE CFC-113 mixing ratios at Cape Grim and previous emissions estimates from AFEAS and Rigby et al. (2013) (based on AGAGE in situ data) with uncertainties (green lines). The dashed black line shows the modelled 'best fit' emissions with
615 uncertainties (grey lines). The method used for calculating the upper and lower emission bounds is in the supplementary material.
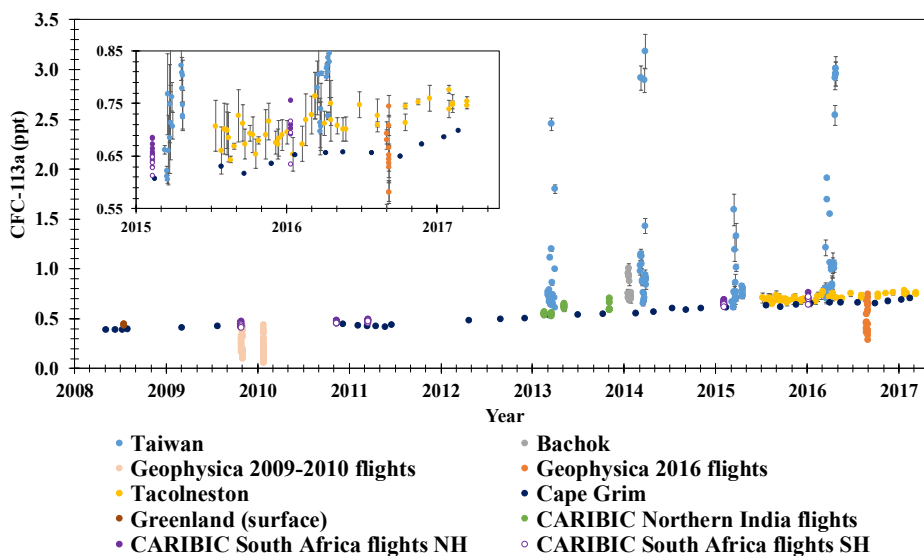
Figure 5. CFC-113a mixing ratios 2008-2017 from all the sources presented in this study with an inset of the period 2015-2017 to give an enlarged view of the Tacolneston data. The error bars represent the 1σ standard deviation.

635

(a) 21/03/2013

(b) 22/03/2014

(c) 30/03/2014

(d) 22/03/2015

(e) 24/03/2016

(f) 25/04/2016

640

(g) 28/04/2016
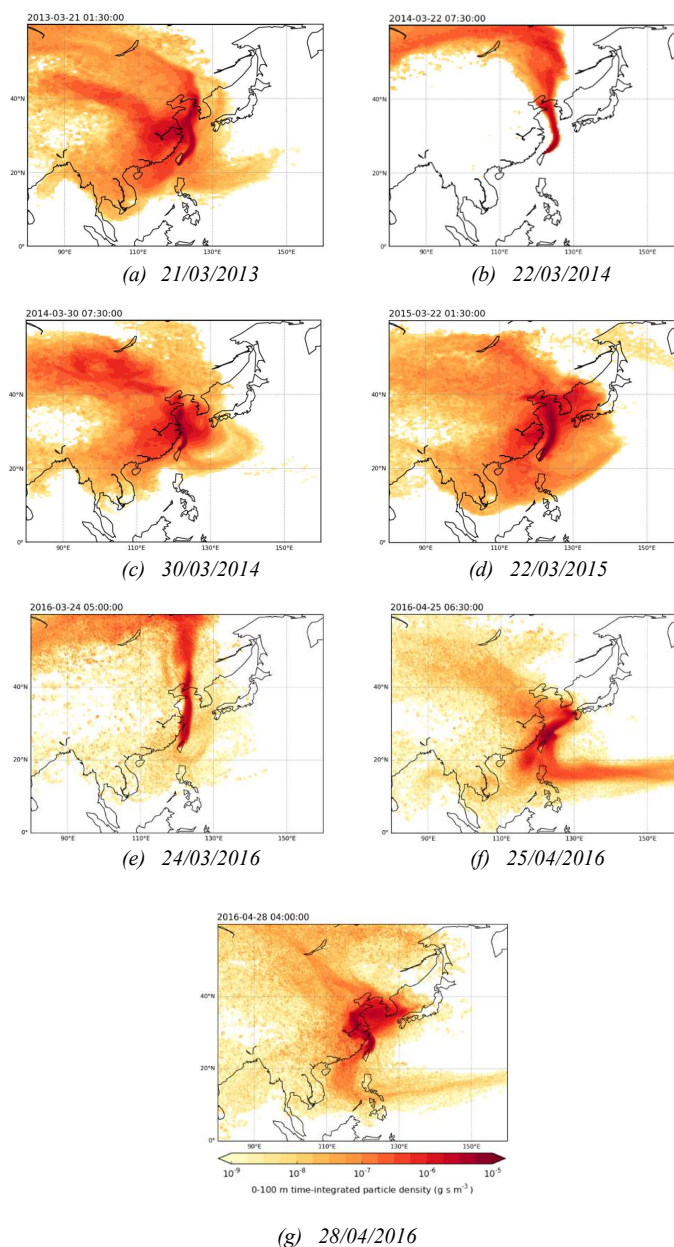
Figure 6. NAME footprints derived from 12-day backward simulations and showing the time integrated density of particles below 100 m altitude for the approximate times when samples were collected during the Taiwan campaign. (a), (c), (d) and (g) are examples of one enhanced CFC-113a mixing ratio in each year. (f) is the
645   sample taken just before (g) when the air was coming from a different direction and the mixing ratio of CFC-113a was much lower. (b) and (e) are also examples of samples with lower CFC-113a mixing ratios. Arrows in Fig. 7 show the mixing ratios of CFC-113a for these NAME footprints. For the rest of the NAME footprints see the supplementary material.
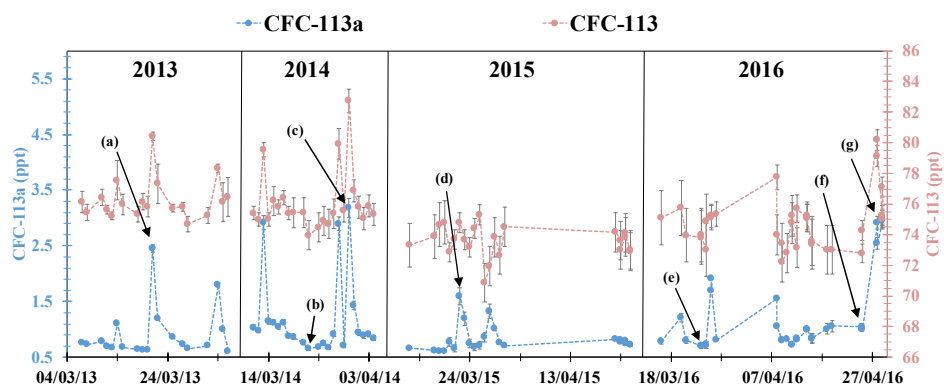
650   Figure 7. CFC-113a and CFC-113 mixing ratios observed in Taiwan in March and April 2013-2016. Arrows show the mixing ratios of CFC-113a that relate to the NAME footprints shown in Fig. 6. The error bars represent the 1σ standard deviation.

Table 2. Squared pearson correlations (R^2) of CFC-113a mixing ratios with other compounds in Taiwan 2013-2016.

	2013	2014	2015	2016
CFC-113	0.866	0.919	0.013	0.429
HCFC-133a	0.923	0.922	0.891	0.637
HFC-134a	0.007	0.049	0.010	–
HFC-125	0.319	0.219	0.016	0.850
CFC-114a	–	–	0.754	0.386
HCFC-123	–	0.010	0.217	0.202
HCFC-124	–	0.529	0.833	0.078
No. of data points	19	23	23	33

655
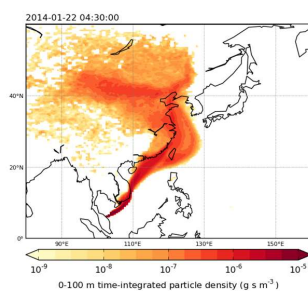
Figure 8. NAME footprint derived from 12-day backward simulation and showing the time integrated density of particles below 100 m altitude on 22/01/2014 during a period of elevated CFC-113a mixing ratios at Bachok, Malaysia.

660